Journal of Applied Polymer Science

Thermal aging and accelerated weathering of PVC/MMT nanocomposites: Structural and morphological studies

Joanna Pagacz,[1] Michał Chrzanowski,[2] Izabella Krucińska,[2] Krzysztof Pielichowski[1]
[1]Department of Chemistry and Technology of Polymers, Cracow University of Technology, 31-155 Krakow, Poland
[2]Department of Material and Commodity Sciences and Textile Metrology, Technical University of Lodz, 90-924 Lodz, Poland
Correspondence to: J. Pagacz (E-mail: jpagacz@chemia.pk.edu.pl)

ABSTRACT: This work focuses on the influence of weathering factors—UV radiation, humidity, and temperature on the structure and morphology of poly(vinyl chloride)/montmorillonite (PVC/MMT) nanocomposites obtained by melt blending. It has been observed that organically modified MMT (OMMT) deteriorates the weathering resistance, the thermal behavior, as well as the long-term stability of PVC. Decomposition of the organic modifier of MMT causes substantial color changes in the PVC nanocomposites as it facilitates the dehydrochlorination process of the polymer. However, the nonmodified MMT provides some stabilization during PVC weathering. The nanocomposites after annealing are characterized by higher glass transition temperature. The increase in heat capacity step (Δc_p) during glass transition suggests that in the PVC composites with nonmodified MMT stronger molecular interactions between the polymer and clay platelets occur than in PVC/OMMT nanocomposites. The scanning electron microscopy images on the surface and the cross section show that thermal aging and weathering proceed by different mechanisms. © 2015 Wiley Periodicals, Inc. J. Appl. Polym. Sci. **2015**, *132*, 42090.

KEYWORDS: clay; degradation; differential scanning calorimetry (DSC); nanostructured polymers; poly(vinyl chloride)

Received 29 September 2014; accepted 6 February 2015
DOI: 10.1002/app.42090

INTRODUCTION

Although virgin poly(vinyl chloride) (PVC) finds numerous applications in construction, electronics, cable, and automotive sectors, it lacks thermal and photochemical stability. To compensate for that, a variety of additives are introduced in the polymer matrix.[1–3] Nanoparticles, especially layered silicates, have attracted great interest as fillers for this purpose. Ishida *et al.*[4] and Wang *et al.*[5] reported first on the preparation of PVC/montmorillonite (PVC/MMT) systems. Melt blending is the most common method for the preparation of PVC nanocomposites[6–8]; however, some articles report on solution blending[9,10] and polymerization in the presence of MMT.[11–13] Layered silicates improve thermal and mechanical properties and significantly reduce flammability, as evidenced by reduced heat release rate, low production of smoke, and low emission of volatile decomposition products. The improvement depends mainly on the proper combination of organoclays modified with different organic salts or polymers, the composition of conventional additives (plasticizer, stabilizer, and flame retardant), and the fabrication route.[14,15]

The behavior of materials under natural and artificial conditions is determined by several factors. Complex PVC products are usually exposed to a variety of weather conditions, such as sunlight, temperature changes, and rain/snow fall. Often the experiments are held in artificial simulated environments to reduce testing time, but one should bear in mind that the results may differ from those on natural conditions due to interactions between atmospheric agents and additives in the stabilized PVC materials.[3] The chemical and physical aging mechanisms of polymer degradation may operate simultaneously: the former affects mainly the molecular structure of polymer, while the physical processes are related to the diffusion of the additives toward the surface.[16] The weathering of the PVC formulations induces dehydrochlorination reactions, photooxidation, and crosslinking, which results in significant modification in the molecular structure of PVC. Under environmental conditions, the degradation consists of a stepwise flow out of inorganic components and plasticizer, while in thermal aging conditions, the rearrangement and aggregation of the molecular chains due to annealing are considered as the main factor of the degradation.[17–21]

The biodegradation process can be studied with tests in which the specimens are buried in soil, compost, or landfill (burial tests). Several reports on behavior of the PVC in landfill proved

Additional Supporting Information may be found in the online version of this article.

that during composting, phthalates and other additives are released from PVC. Additionally, microbial growth was identified in plasticized PVC.[22,23] The physical and morphological characteristics of weathering mechanism of PVC have been studied in detail but most of the previous studies focused on blends (PVC with processing additives) or commercial products (e.g., window profiles and tubes). However, there are only a few articles dealing with the weathering of PVC-based nanocomposites.[24–28] We have previously reported that sodium MMT can affect the long-term behavior of PVC materials in soil.[29] Our preliminary studies on the thermal and artificial weathering of PVC/MMT nanocomposites prepared by melt blending showed that temperature above 125°C has only slight influence on the structure.[30]

In this article, we study PVC/MMT nanocomposites containing processing additives and two types of MMT, fabricated by melt blending. The main objective is to study the morphological and structural changes, caused by different weathering conditions, in plasticized PVC systems.

We show that organically modified MMT incorporated through melt blending worsen the PVC stability, while the sodium MMT practically has no influence on the PVC blend behavior under testing conditions. The proper choice of additives and method of preparation strongly influence the final properties of PVC/MMT nanocomposites.

EXPERIMENTAL

Materials

Suspension poly(vinyl chloride) with *K* value 67 and viscosity value 110 mL/g, Polanvil S-67 HBD (**PVC**—Zaklady Azotowe ANWIL S.A., Poland), commercial nanoclays: sodium montmorillonite (**Na**—Süd Chemie, Germany) and MMT modified by benzyldimethyloctadecylammonium chloride with trade name Nanofil® SE3010 (**SE**—Süd Chemie, Germany) were used. The other additives were as follows: plasticizer—dioctyl phthalate (**DOP**—Zaklady Azotowe Kedzierzyn S.A., Poland), stabilizer—calcium stearate (Boryszew ERG S.A., Poland), chlorinated flame retardant—chloroparaffine (Konimpex, Poland), flame retardant—aluminum hydroxide, known as Alfrimal 103 (**ATH**—Alpha Calcit Füllstoff GmbH & Co. KG, Germany), and compatibilizer/plasticizer—epoxidized soybean oil Ergoplast ES® (Boryszew ERG S.A., Poland). All the materials were dried before use: sodium MMT at 100°C for 24 h, Nanofil® SE3010 at 80°C for 24 h, PVC and other additives at 40°C for 4 h.

Sample Preparation

The basic composition of PVC blend was calculated for PVC powder: 40 phr of DOP, 2 phr of calcium stearate, 3 phr of epoxidized soybean oil, 5 phr of chloroparaffine, and 25 phr of aluminum hydroxide (ATH). The composites contain additionally 3 phr of two different nanofillers: sodium MMT (PVC/Na) and organically modified MMT (PVC/SE).

First, MMT was co-intercalated with dioctyl phthalate (DOP) at 80°C in a laboratory mixer (2000 rpm) for 1 min. The stabilizer and flame retardants were then added and mixed for 2 min. After that, PVC and compatibilizer were added and mixed for additional 10 min. The homogenous mixture was processed in a

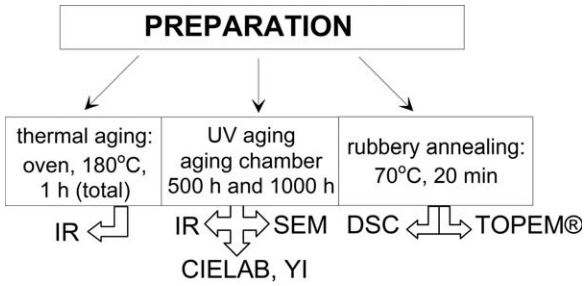

Scheme 1. Methods for aging tests of PVC materials.

HAAKE MiniLab II Micro Compounder. The temperature was maintained at 134°C for the PVC/SE nanocomposites and 145°C for the PVC/Na one. These—relatively low—temperatures were chosen to prevent polymer degradation due to local heating, caused by shearing. The screw speed was maintained at 70 rpm. The melt circulated into the extruder's backflow channel for 1 min (PVC/SE) or for 2 min (PVC/Na) to improve homogeneity. Strips with thickness 1.7 ± 0.2 mm and width 4.5 ± 0.5 mm were produced.

Weathering Techniques and Characterization

Samples after preparation were subjected to several weathering and thermal procedures (Scheme 1).

Thermal Aging. Thermal aging of PVC nanocomposites was performed in a laboratory oven at $180°C \pm 0.5°C$ in air. Strips with dimensions of about 2.0 mm × 4.5 mm × 60 mm were placed on an aluminum foil inserted in the oven, and then every 10 min over a period of 1 h one of them was removed, photographed, and subjected to Fourier-transform infrared spectroscopy (FTIR) analysis.

Artificial Weathering of PVC/MMT Nanocomposites. Ultraviolet (UV) exposure tests were carried out in an Atlas WOM Ci 4000 weathering device (Atlas Material Testing Technology LLC), according to PN-EN ISO 4892-2:2013-06 standard. The tester is equipped with Xenon lamps, characterized by radiant exposure with maximum of irradiance at $\lambda = 340$ nm filtered with two borosilicate filters. It provides good simulation of an outdoor exposure by several environmental factors such as sunlight, temperature, and rain.

The test specimens cut in 110 mm × 5.0 mm × 1.7 mm strips, were mounted in a similar position to the radiation source on the rotating cylindrical sample rack with a solid backing, which avoids any differences in the irradiation distribution on the specimen surface. The specimens were then subjected to 500 and 1000 h of accelerated weathering. Two cycles to stimulate day and night conditions were performed. The parameters were chosen as follows (Table I).

After this procedure, the samples were imaged by scanning electron microscopy (SEM) and their FTIR spectra were recorded. In addition, yellowness index (*YI*) was estimated according to ASTM E313-98 standard, and color changes were determined in the Commission International d'Eclairage three-dimensional color space (CIELAB). Details about these techniques will be

Table I. Set of Weathering Conditions

Period	Irradiation (W/m^2)	Time (h)	BST (°C)	CT (°C)	Humidity (%)	Spray of water
Light	70	4	60	40	45	18 min/102 min dry
Dark	0	2	50	50	75	18 min/102 min dry

BST, black standard temperature; CT, chamber temperature.

provided later in section "Color Characterization of Irradiated Samples."

Rubbery Annealing (DSC). The rubbery annealing effect[31] was studied in a Mettler Toledo DSC823^e calorimeter cooled with intracooler and calibrated with indium and zinc standards. The samples were cut to thin foils and sealed in aluminum crucibles under static air atmosphere. Initially, DSC thermograms were recorded with the pristine materials in the range of 25–170°C at 4°/min. To study effects of rubbery annealing, we subjected fresh samples to the following temperature protocol:

1. heating to 70°C at 20°/min (to anneal the sample above its T_g)
2. rubbery annealing at 70°C for 20 min to allow for partial crystallization[32]
3. cooling to room temperature and heating up to 170°C at 4°/min, to observe changes in material after annealing (DSC measurement).

Samples after rubbery annealing (segment 2) were also subjected to DSC measurements with stochastic temperature modulation (TOPEM® METTLER TOLEDO 823^e DSC).[33] This method analyzes dynamic behavior of materials during one single measurement with multifrequency modulation. The underlying constant heating rate is superimposed with the random temperature perturbations and after Fourier transformation, it is possible to calculate the quasi-static heat capacity $c_{p,0}$, the frequency-dependent complex heat capacity, $c_p^*(\omega)$, and the nonreversing heat flow $\Phi_{non\text{-}rev}$. The reversing component is calculated from the quasi-static heat capacity. The method needs to use sufficiently low heating rate (0.01–2°/min) and small values of temperature perturbation δT_0 (1 mK–0.5 K).

The following parameters were chosen: underlying heating rate: 2°/min, amplitude of the temperature pulse: ±0.25 K, switching time range (which limits the duration of the pulses): minimum 15 s and maximum 30 s, and sample weight: about 17 mg. Except the different heating rate and temperature range in the final run, the thermal protocol is the same as with the conventional DSC experiments.

Morphological Characterization. The morphology of PVC/MMT nanocomposites and neat PVC after artificial weathering was evaluated by a digital camera and SEM. A scanning electron microscope TESCAN type VEGA II SBH with an energy dispersive X-ray spectrometer (EDXS) (Oxford Instruments Inca Penta FETx3) was used to observe coated sample surfaces in low vacuum and for the general quantitative and qualitative analysis on micro areas of PVC/MMT nanocomposites. Besides, the bulk observation of nonweathered materials (foil ca. 1 mm of thickness) was performed with SEM FEI XL30 in low vacuum conditions (the surface was covered with gold, accelerating voltage 10–20 kV).

Structural Characterization (FTIR). Fourier-transform infrared (FTIR) spectra were recorded with a Perkin Elmer Spectrum 65 spectrophotometer in ATR mode with C/ZnSe crystal; four scans with resolution 4 cm^{-1} in the wave number range of 600–4000 cm^{-1} were performed. For each sample 10 spectra were performed on the exposure surface. Baseline correction and normalization (with respect to the C—H absorption at 2959 cm^{-1}) were applied for the averaged IR spectra. The polyene sequence index (*PI*) was calculated according to eq. (1):[26]

$$PI = \frac{\text{absorbance}_{C=C}}{\text{absorbance}_{2959}}, \quad (1)$$

where absorbance$_{C=C}$ – absorbance of polyene at 1597 or 1652 cm^{-1}.

Color Characterization of Irradiated Samples. An SP64 Portable Sphere Spectrophotometer was used to measure the

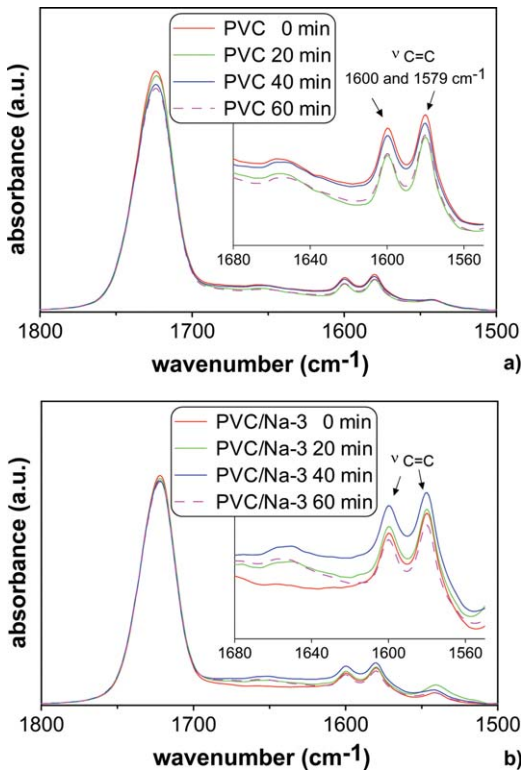

Figure 1. FTIR spectra of PVC (a) and PVC/Na-3 nanocomposite (b) before (0 min) and after 20, 40, and 60 min of thermal weathering in the range of 1500–1800 cm^{-1}. [Color figure can be viewed in the online issue, which is available at wileyonlinelibrary.com.]

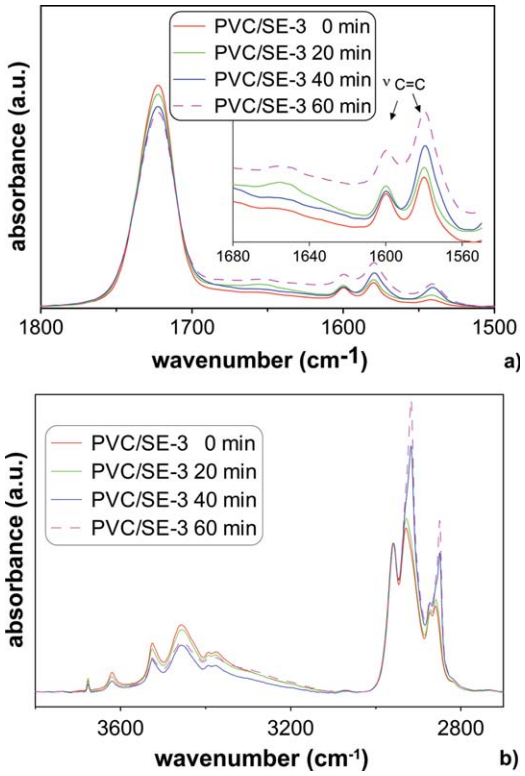

Figure 2. FTIR spectra of PVC/SE-3 nanocomposite before (0 min) and after 20, 40, and 60 min of thermal weathering in the range of (a) 1500–1800 cm^{-1} (b) 2700–3800 cm^{-1}. [Color figure can be viewed in the online issue, which is available at wileyonlinelibrary.com.]

yellowness index, according to the procedure described in ASTM standard E313-98 and the color differences by using the Commission International d'Eclairage three-dimensional color space (CIELAB 1976 color space). In this system, three colorimetric coordinates (color values) of Y and Z from the CIE Standard Color Table have been transformed into three new values of coordinates: *L*, *a*, and *b*. CIELAB system allows calculating color differences that correlate with perceived magnitude of color difference by the average observer. The change in the color value is characterized as a difference between values for the sample after weathering and the standard (sample before weathering).[34] The color values were calculated on the basis of reflectance data obtained during scanning of the sample surface in the wavelength range 400–700 nm using SCI method with accuracy of 0.10 of total color deviation (ΔE_{ab}) on white ceramic standard. The measurements conditions were: angle observer: 10°, illuminant: D65, size of the mask: 8 mm measurement area/13 mm of target window.

Yellowness index (ASTM E313) is a number calculated from spectrophotometric data that describes the change in color of a test sample toward yellow, what correspond to polyene sequence formation [eq. (2)]:[35]

$$YI = \frac{0.72a + 1.79b}{L} \cdot 100. \quad (2)$$

This parameter allows to evaluate color changes in a material caused by real or simulated outdoor exposure. It has also been used to determine the influence of different PVC composition and organic modifier of MMT on the thermal stability of PVC.[24,25,36]

RESULTS AND DISCUSSION

Thermal Aging

Structural Changes During Thermal Aging. The heat treatment causes evaporation of volatile compounds and decomposition of less-stable organic additives like the MMT modifier. The FTIR spectra of the matrix and the nanocomposites before and after thermal aging are illustrated in Figures 1 and 2. The differences in the material after thermal weathering are visible in the intensity of absorbance peaks. The spectra are complex due to overlapping of the bands coming from the polymer and additives.

The main spectral changes for the neat PVC can be observed in the region 1500–1800 cm^{-1} [Figure 1(a)]. The absorbance peak around 1650 cm^{-1} corresponds to polyene sequences present in the polymer macrochain, and its presence denotes partial degradation already during processing.[3] Progressive weakening of the carbonyl band at 1724 cm^{-1} and double band at 1579 and 1600 cm^{-1}, from conjugated C=C vibrations in aromatic ring of plasticizer, suggests evolution of the phthalate plasticizer.[37] Besides, different species formed during thermal aging can influence the area of carbonyl peak, but there is no dependence on the area of carbonyl peak and time of aging (Table II). This suggests that products of thermal degradation can react subsequently themselves and favor crosslinking of the polymer chain.

The spectra of PVC nanocomposites [Figures 1(b) and 2] present effects similar to those of the reference blend. The progress of degradation is reflected on the gradually increasing intensity of the bands corresponding to unsaturated, isolated polyene structures (ca. 1650 cm^{-1}) and conjugated double bonds (1579 and around 1600 cm^{-1}) [Figures 1(b) and 2(a)].[38]

Formation of conjugated polyene sequences causes yellowing of material and evidences both, dehydrochlorination process and formation of aromatic compounds.[18,26,39,40] Contrary to the PVC blend, we may observe [Figures 1(b) and 2(b)] small increase in the intensity of the bands corresponding to hydroxyl group vibrations at 3100–3600 cm^{-1}. These groups come from ATH particles, epoxidized soybean oil, and nanofillers as well. Decomposition of organic modifier of MMT causes the visible

Table II. Integral Intensities and Areas of Carbonyl Band for Different Time of Aging of PVC Materials

Time of thermal aging (min)		0	20	40	60
Intensity	PVC	1.83	1.80	1.71	1.67
	PVC/Na-3	2.72	2.68	2.66	2.64
	PVC/SE-3	2.65	2.54	2.40	2.33
Area	PVC	1.85	1.89	1.51	1.653
	PVC/Na-3	2.15	1.77	2.13	1.68
	PVC/SE-3	2.37	2.09	1.84	1.88

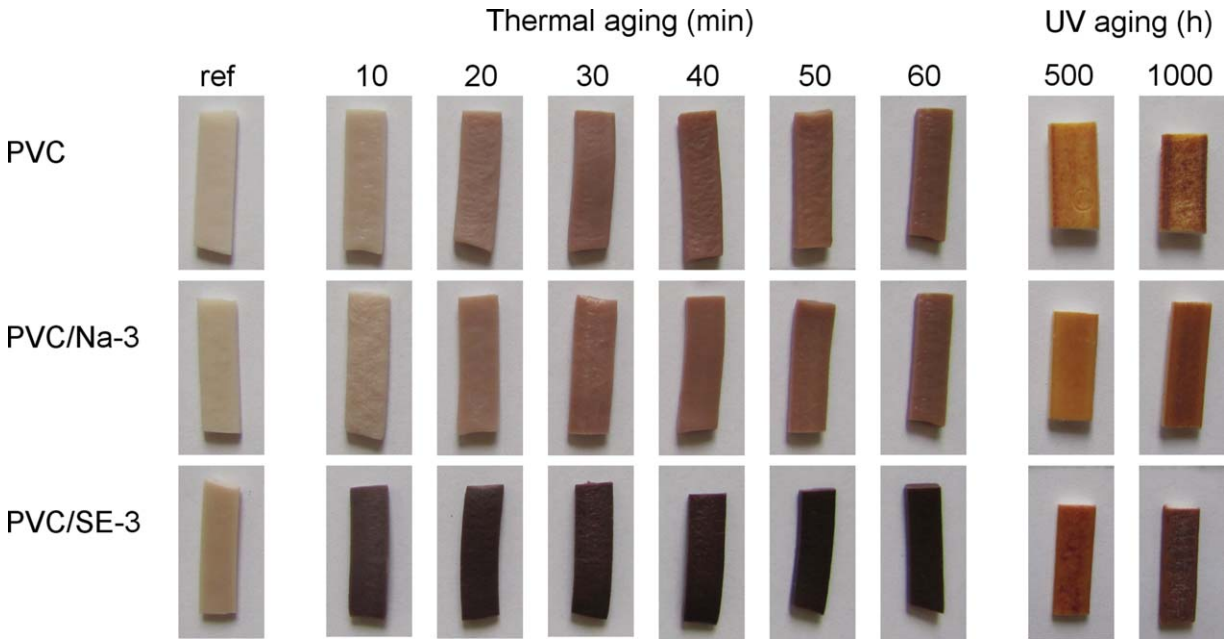

Figure 3. Photographs of PVC and its nanocomposites before and after thermal and UV aging. [Color figure can be viewed in the online issue, which is available at wileyonlinelibrary.com.]

changes in the range of C—H vibrations (2800–3000 cm^{-1}) and suggest scission of polymer macrochains [Figure 2(b)]. On the other hand, loss of the chlorine atoms is reflected as a decrease of the band at 690 cm^{-1}, assigned to C—Cl stretching vibrations.

Furthermore, a small decrease in the 3000–3600 cm^{-1} region, which correspond to hydroxyl group vibration in ATH, clay, calcium stearate and epoxidized soybean oil [Figure 2(b)], is observed. Meanwhile, only slight changes in the same region for PVC resin and PVC/NaMMT nanocomposites were recorded. These differences can be related to the fact that hydroxyl groups can trap macroradicals of PVC through chemical reactions and thus limit oxidation process.[26]

The polyene index, calculated as an absorbance at 1579 and 1652 cm^{-1} divided by the absorbance of the reference band at 2959 cm^{-1} [according to eq. (1)], represents the extent of polyene species formation. When considering the polyene index for PVC the values are practically the same during thermal treatment, while PVC nanocomposites are characterized by significant changes in the *PI* values (see Supporting Information Figure S1).

As for PVC/Na-3 nanocomposite a progressive increase of *PI* 1579 value can be distinguished, for PVC nanocomposite with modified MMT there is no such dependence. At the same time, PVC shows only slight changes during aging experiment. No monotonous dependence for polyene index with time of aging comes from competitive processes of radicals formation and their trapping by specific groups and nanoparticles as well[26] (see Supporting Information Figure S1a). The higher values of polyene index at 1579 cm^{-1} for nanocomposites with modified MMT can be a result of decomposition of ammonium salt. This process occurs according to Hoffmann degradation mechanism and lead to H^+, which accelerate dehydrochlorination of PVC. Random isolated double bonds with allylic chlorine atoms are rather unstable, but according the initiation of the thermal dehydrochlorination of PVC is mainly due to presence of random allylic chlorine atoms or branches with tertiary chlorine atoms.[3] *PI* values at 1652 cm^{-1} (see Supporting Information Figure S1b) suggest that nanocomposites also contain some part of isolated polyene sequences which may come from random elimination of hydrochloride.

The FTIR investigation evidences that OMMT favor degradation of PVC, while nonmodified MMT presents only slight influence on the dehydrochlorination process. Reference PVC material is the most stable material, but trapping agents, such as hydroxyl groups present in the MMT structure, can influence positively the thermal aging process.

Color Changes After Aging. After thermal aging, there are no significant changes in microscopic morphology, but severe discoloration occurs (Figure 3). Materials with modified MMT became violet at the beginning and black after prolonged heating, while nonfilled PVC and PVC filled with Na-MMT presented small changes from beige to pink color. The strong discoloration effect concerns not only the surface exposed but also the bulk material and it comes from degradation of organic modifier of MMT and resulting dehydrochlorination of PVC.[41]

Besides, loss of the plasticizer leaves the surface of PVC shiny after thermal treatment, an effect known in the industry as a blooming process.

Artificial Aging

Photodegradation of PVC usually consists of dehydrochlorination, chain scission, and crosslinking.[3] PVC in its pure form contains C—H, C—C, and C—Cl bonds, so it should not be

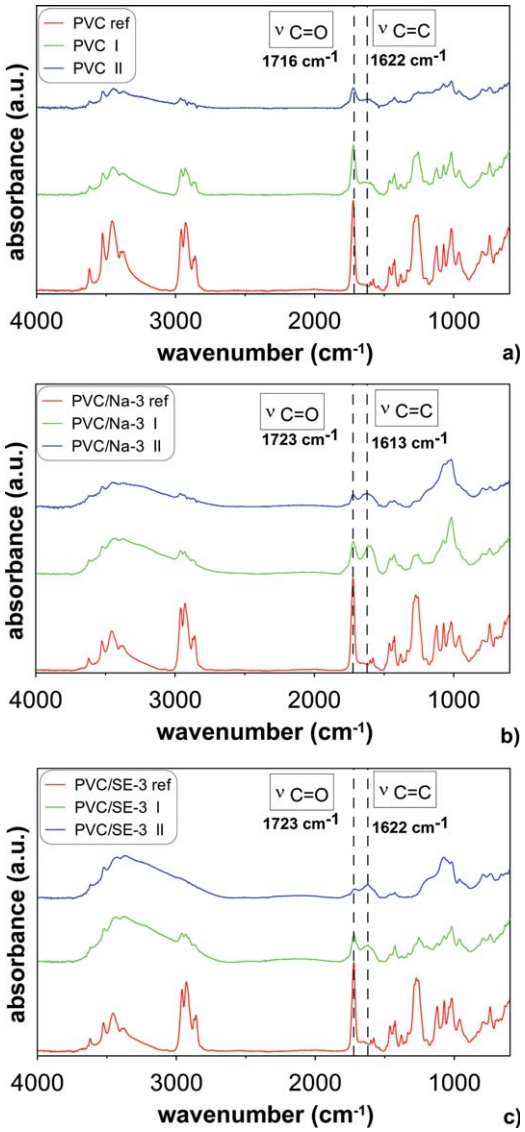

Figure 4. IR spectra of samples after UV weathering: (a) PVC, (b) PVC/Na-3, (c) PVC/SE-3 (I, 500 h; II, 1000 h). [Color figure can be viewed in the online issue, which is available at wileyonlinelibrary.com.]

degraded by UV radiation as these groups do not absorb UV from daylight spectrum. However, several additives, e.g., solvents left inside PVC particles, can act as sensitizers. The most significant are unsaturated bonds, which can participate in several reactions leading to formation of radicals and then to carboxylic groups, which absorb daylight UV radiation and initiate photodegradation. Regarding C—Cl bond the chlorine radicals may be formed and then the radicals may react with a neighboring hydrogen. Therefore, photodegradation can be initiated by imperfections present in the polymer structure, which limits the process mainly to the amorphous part of the polymer.

In the PVC products, three main failure modes can be observed: yellowing caused by polyene formation, fading due to degradation of polyenes, which involves breaking of double bond and oxidation reactions, and chalking. The oxidative products, like for example peroxides, may cause further scattering and hazing. The last possible failure is chalking and it is a result of progressive yellowing, fading, and decreasing of surface integrity. It leads to formation of cracks and flaking of the surface.[42]

Changes in the Structure of PVC/MMT Nanocomposites (FTIR). The spectra in Figure 4 show that the UV irradiation caused structural changes—specimens after exposure exhibit broadened absorption bands with time. The results are in good agreement with previous studies on PVC blends.[43,44]

The most significant changes can be observed in the region of carbonyl group (1723 cm^{-1}), and C—C vibrations of benzene ring in the plasticizer molecule (1579 and 1600 cm^{-1}) (Figure 4). The band in 1560–1660 cm^{-1} range is assigned to conjugated polyene species.[38] Broadening of the carbonyl band at around 1723 cm^{-1} indicates that different types of groups were created upon UV exposure, such as —COCl groups which give a weak band at around 1785 cm^{-1}.[3,45] When PVC is irradiated, the IR spectra also exhibit broadening of absorbances at 3455 cm^{-1} characteristic of OH groups, which are related to the formation of degradation products (e.g., acids, alcohol, and peroxides). Furthermore, the band at about 1025 cm^{-1} assigned to Si—O stretching vibrations became more visible in the IR spectra of nanocomposites, probably due to accumulation of inorganic ingredients in the outer layer of material.

The spectra are complex because photooxidation leads to several different compounds, such as alcohols, aldehydes, chloroorganic compounds, esters, and ketones, which can give new radicals initiating subsequent reactions.[46]

Deterioration changes are observed along time of the exposure as indicated by broadening and disappearing of the characteristic bands. This may be a result of photooxidation process, as well as damaged surface of material during weathering, as

Table III. Color Differences and Haze Values of PVC and PVC/MMT Nanocomposites

	Differences in color parameters								Haze value	
	ΔE		ΔL		Δa		Δb		h (°)	
Sample	I[a]	II[b]	I	II	I	II	I	II	I	II
PVC	32.57	28.03	−25.05	−24.50	15.82	9.82	13.53	9.44	47.77	52.65
PVC/SE-3	41.21	42.00	−36.79	−41.14	16.72	8.45	8.10	−0.61	46.19	45.97
PVC/Na-3	34.45	44.15	−23.06	−40.64	13.97	13.76	21.45	10.39	62.19	50.01

[a] I, 500 h of weathering.
[b] II, 1000 h of weathering.

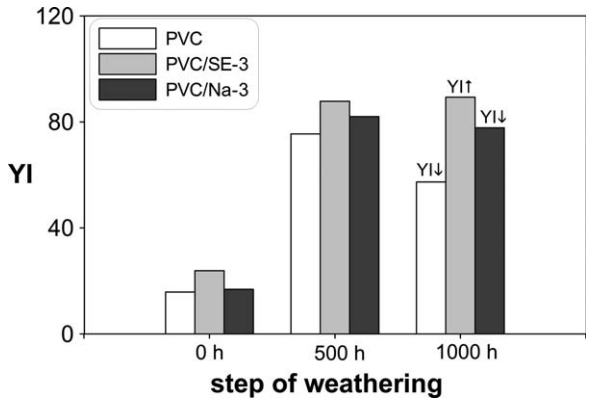

Figure 5. Yellowness index of PVC and its nanocomposites.

observed on the SEM microphotographs to be shown in the next paragraph.

Color Characterization and Yellowness Index Determination. Color changes of PVC samples, upon artificial weathering, were described by coordinates $L^*a^*b^*$ (and $L^*C^*h^\circ$) and by the yellowness index. A shift in color can also be calculated as the total color deviation – ΔE^*_{ab} or as the shift in the yellowness index value – ΔYI. In Table III delta values of color coordinates are given.

Comparing the lightness with yellow coordinate before and after weathering experiment, one can observe that the color differences in nanocomposites are much higher than those for pure PVC. Materials with organo-modified MMT became darker, similar to the PVC/Na nanocomposites after 1000 h of weathering, but less yellow than reference blend and PVC/Na nanocomposites. This means that UV weathering induces different processes in the nanocomposites related to their composition.

Moreover, the nanocomposites exhibited darkening (higher ΔL values) and more intense discoloration (higher ΔE values) than PVC after weathering, in agreement with earlier studies.[45] Besides, the plasticizer—which contains carbonyl groups effectively absorbing UV light—can increase the darkening rate because of production of free radicals and color changes in the plasticizer itself.[47]

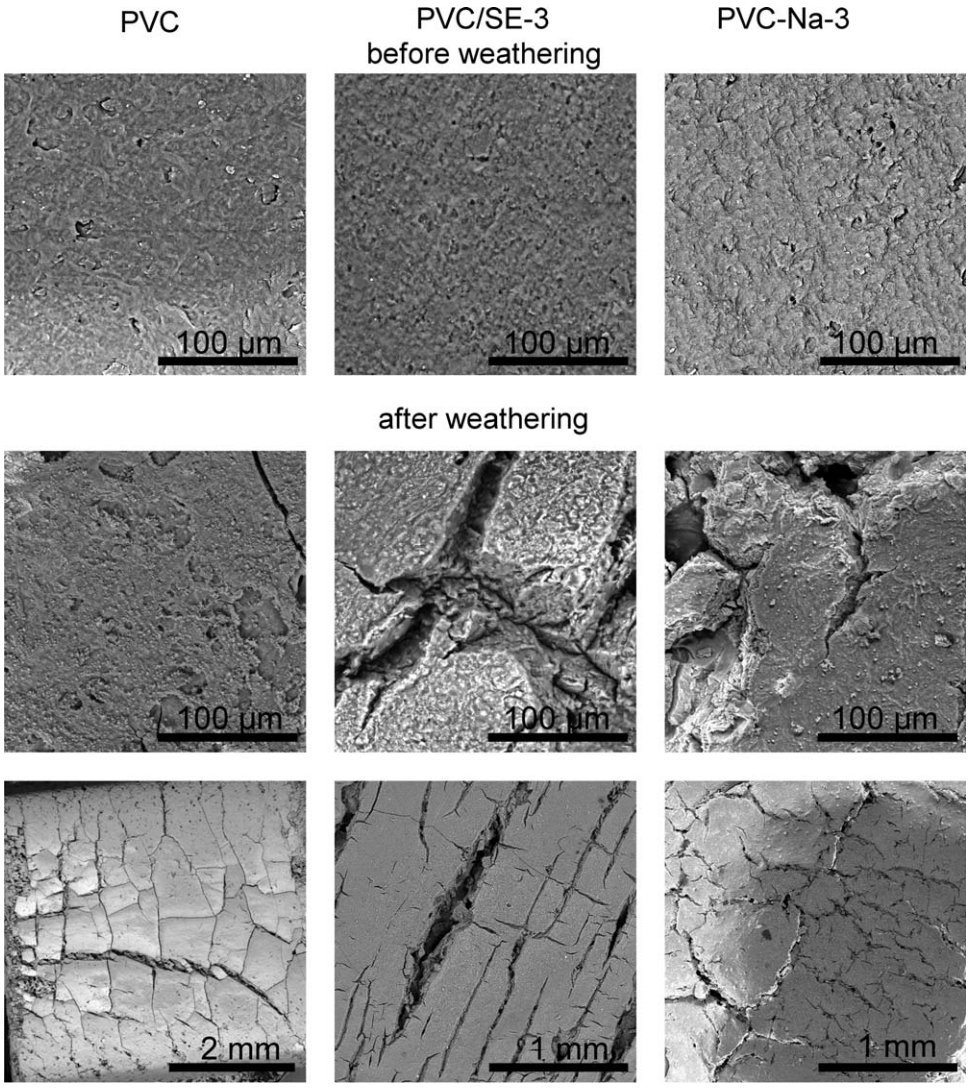

Figure 6. SEM microphotographs of surface of PVC and its nanocomposites before and after 1000 h of weathering.

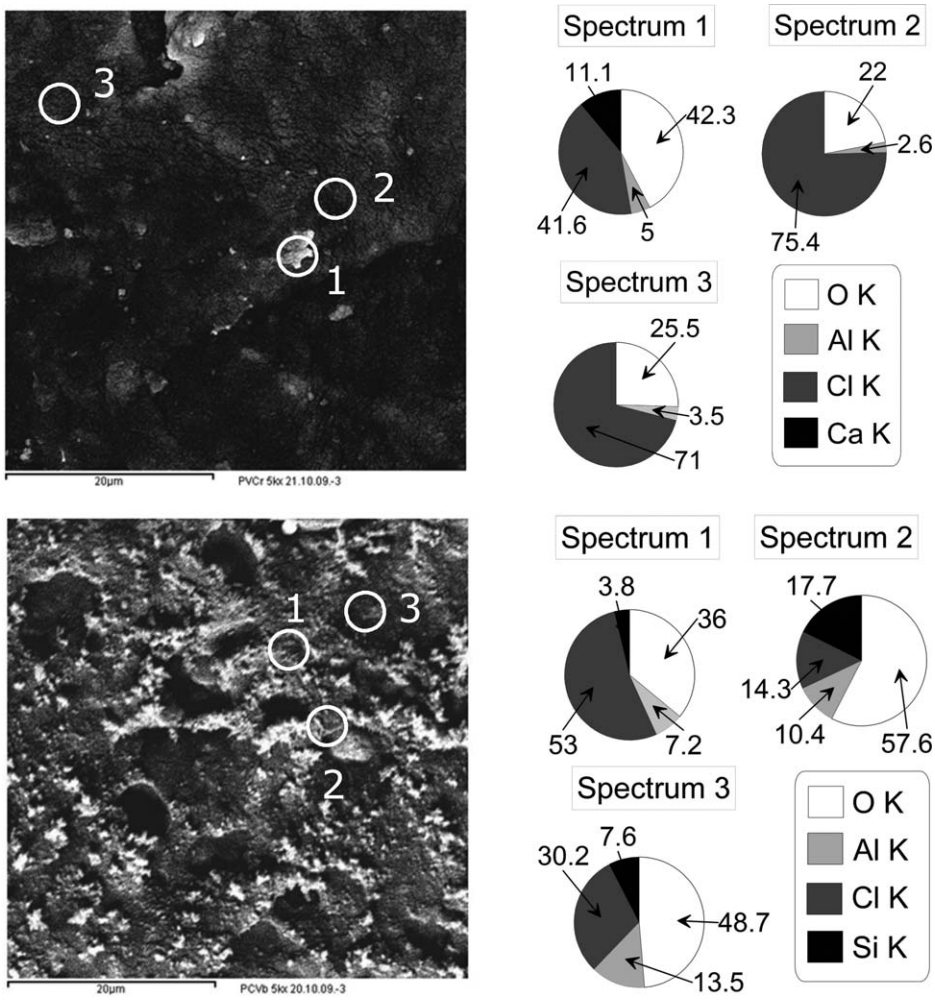

Figure 7. Morphology and composition analysis on micro areas of PVC before (up) and after 1000 h of weathering (down).

The reasons for yellowing of PVC materials have been discussed in Ref. [15] and it was suggested that yellow color comes from dehydrochlorination, initiated during processing, and continued during photodegradation. The formation of conjugated double bonds–polyenes leads to yellowing and darkening of PVC and its nanocomposites upon aging experiments. Additionally, photobleaching mechanism can be distinguished concerning the cyclohexadiene formation in polyene sequences.[48,49]

The extent of the discoloration expressed by yellowness index (an average value from three measurements) and difference of $YI - \Delta YI$ is presented in Figure 5.

The MMT addition causes color shift, depending on the clay content and the presence of organic modifier in MMT structure.[24,25,41] Two distinct trends as a function of MMT chemistry can be found. The results for PVC and its nanocomposites with nonmodified MMT indicate differences with the irradiation time: longer irradiation time causes darkening of the material and decrease of the *YI*. The PVC/SE materials show different behavior—*YI* increases slowly with irradiation time, which may indicate photobleaching of the material. Some experiments showed that color change in PVC materials depends on the radiation used: if sun radiation is used PVC undergoes simultaneously two different processes—yellowing and photobleaching.[50,51] This is in accordance with CIELAB coordinate values obtained for PVC/MMT nanocomposites.

On the other hand, the processing additives used in PVC/MMT nanocomposites' formulation can influence the *YI* value, as it has been reported by Karmalm *et al.*[52] The synergistic effect of the epoxidized soybean oil and calcium stearate is a very interesting topic for further weathering studies.

Morphological Changes (SEM). In the case of UV-irradiated samples the color changed from light beige to brown with irradiation time, which indicates that photo-dehydrochlorination may have occurred (Figure 3). Artificial conditions cause color changes, which are due to the formation of long polyene sequences inside the thin layer on the surface exposed to UV light.[45]

SEM experiments, performed on the samples before weathering tests, showed that the extruded materials have porous structure, which can influence the thermal and weathering behavior.[30] Nonmodified PVC has a more homogenous and smooth surface, while the nanocomposites, especially with OMMT, present several cavities, in agreement with earlier studies.[53] The surface

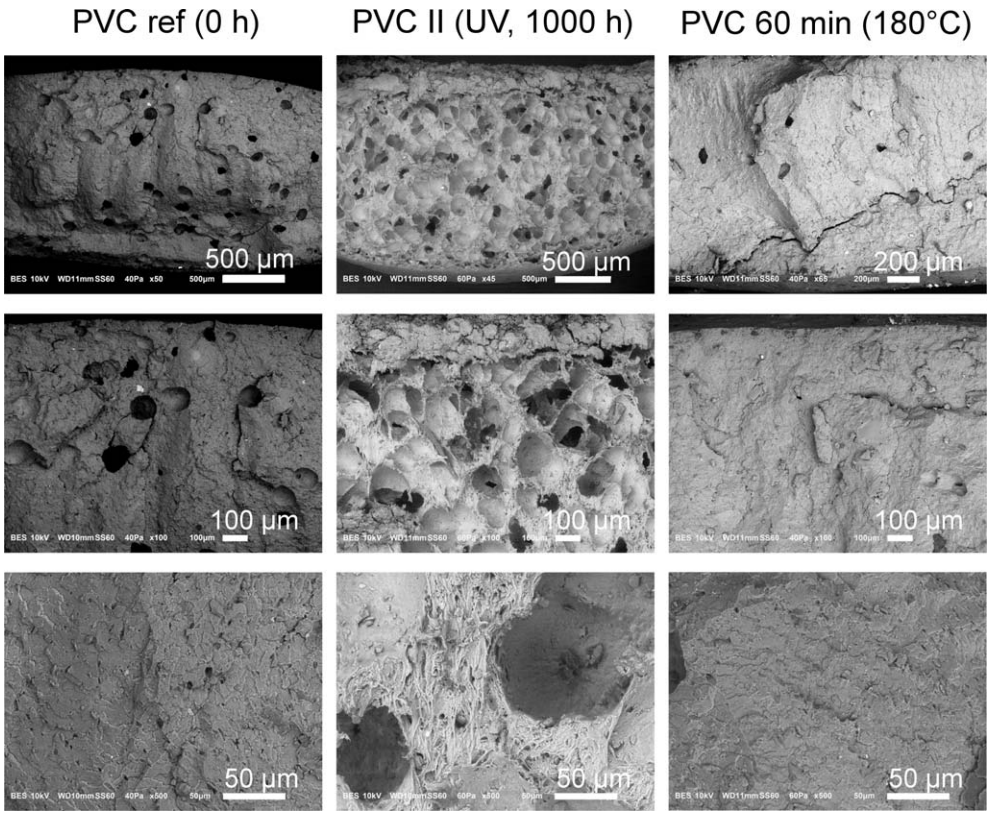

Figure 8. The cross section of PVC before and after thermal aging and weathering.

morphology before and after UV irradiation is shown in Figure 6.

Upon accelerated weathering, PVC materials are known to undergo slow surface erosion, which leads to a granular and mineral-rich surface.[17] Plasticizer is lost first, as the most volatile additive in PVC formulation, and its loss depends on its compatibility with the polymer matrix. According to previous investigations,[20,35,54] plasticizer migrates through the material and forms a sticky layer on the surface, and is lost by migration and evaporation. Besides, the formation of cracks increases porosity of material and thus opens the PVC structure to a more extensive diffusion of oxygen.[3]

Following these observations, it may be concluded that samples present considerable changes in texture of the surface after the weathering process. SEM images show a development of microcracks on the exposed surface of material. It can be observed for material with OMMT addition that cracks run parallel to the direction of extrusion, which may indicate that they develop through enlargement of imperfections on the surface of material. On the other hand, composites with nonmodified MMT are characterized by less cracked surface, which suggest that they provide slight stabilization (Figure 6).

On the other hand, the EDXS composition analysis (Figure 7) proved that alumina trioxide and silica oxide accumulate on the surface of weathered materials, forming a mineral-rich surface. This fact stays in accordance with the assumption that during weathering, inorganic components migrate to the surface of composite. Moreover, the additives may be washed up by water used for sample spraying, and some of them may contaminate other samples in the testing chamber.

The influence of water on the weathering behavior of PVC was tested in detail in articles[42,55,56] and it may be conclude that the presence of water favors formation of oxidation products and the weathering itself. The hydroxyl radicals interact with unsaturations in the polymer derived from photodegradation, what results in whitening of the surface. This process competes with yellowing of PVC and thus variability of the measured *YI* values is observed (Figure 5). A second influence of water on degradation may be that it removes the degraded layer, uncovering more uniform regions of the sample, with lower amount of conjugated double bonds.

Here, the effect of water or humidity was not tested because the main object of the research was UV and temperature influence on the PVC materials, and there is no pigment in the PVC composition which may promote radical formation. However, the composites in the water absorption test[57] showed higher values of water absorption than the reference (0.68%)—for PVC/Na-3 the water absorption was almost 1.84% and for PVC/SE-3, 1.43%.

It is known that moisture primarily affects the gloss and haze of materials and can accelerate the weathering process. The haze values, provided by spectrophotometric measurements (Table

Table IV. Key Thermal Properties for Glass Transition (DSC) and Melting Obtained by DSC (4°/min) and TOPEM® (2°/min) Analyses

			T_m (°C)		ΔH_m (J/g)	
Sample	T_g (°C)	Δc_p (J/g K)	DSC	TOPEM®	DSC	TOPEM®
PVC nonannealed	56	0.138	109	111	1.26	1.15
PVCa annealed	75	0.084	109	112	1.42	0.74
PVC/Na-3 nonannealed	55	0.146	113	112	1.32	1.20
PVC/Na-3a annealed	83	0.060	113	114	1.47	1.18
PVC/SE-3 nonannealed	55	0.160	105	108	0.83	0.85
PVC/SE-3a annealed	77	0.060	107	110	0.87	1.05

T_g, glass transition temperature; Δc_p, change in heat capacity during glass transition; T_m, melting temperature; ΔH_m, enthalpy consider to endothermal effect—melting process (in TOPEM® evaluated from total heat flow curve).

III), decreased after weathering from 70 for PVC and about 80 for composites to values varied in the range of 45–62. However, the highest change was observed for composites with modified MMT, what may suggest the stronger influence of moisture on this kind of material.

Also, the tensile loads produced during processing can accelerate moisture uptake by opening existing internal cavities or by influencing on the microcrack formation.

Degradation Mechanism of PVC/MMT Nanocomposites

Comparing the two main types of artificial aging on the plasticized PVC/MMT nanocomposites, weathering and thermal aging, a few conclusions are derived. Artificial conditions cause color changes, which are due to the formation of long polyene sequences, while during the thermal treatment samples discolor due to decomposition of organic modifier inside MMT's structure.[41] Under weathering conditions, main mechanism of the degradation was both UV-induced hydrogen subtraction (scission of the C—Cl bond) resulting in free radicals formation and less occurred photochemical oxidation of polyenes. The thermal aging influence on the plasticizer evaporation/blooming and thus makes the bulk material more compact, with much less micropores. Under UV irradiation plasticizer release was also observed[56]; however, the plasticizer loss was clearly visible after 1000 h of weathering. The materials posses cracked brown-colored surface from the side of UV irradiation, and compact skin from nonirradiated side. The core is more porous comparing to the reference material, due to plasticizer.

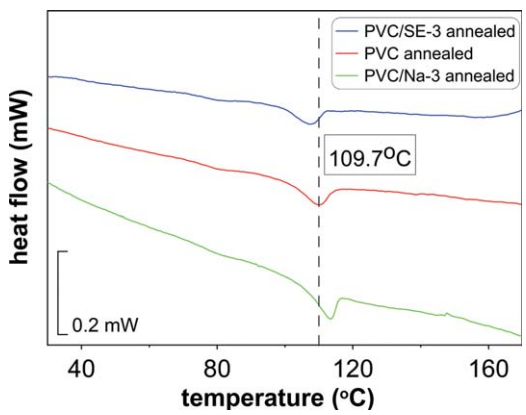

Figure 9. DSC curves of PVC composites after rubbery annealing. [Color figure can be viewed in the online issue, which is available at wileyonlinelibrary.com.]

Figure 8 shows the cross-sectional surfaces after thermal aging and weathering. It is clearly seen that weathering is limited to the certain area of the sample, here approximately 233 μm from the surface. The weathered surface is characterized by different structure, more compact with several cracks, while the core is highly porous with visible fibrillar structures.

Rubbery Annealing

For the nonannealed samples, DSC[57] (see also Supporting Information Figure S2) and TOPEM® thermograms (published in Ref. 58) show two distinct regions: a step around 55°C and a weak endothermal peak around 110°C. The first one corresponds to the glass transition, in agreement with DMA (tan δ peak around 42°C)[57] (see also Supporting Information Figure S3). T_g values (Table IV) are significantly higher than those for PVC plasticized with similar amount of DOP (0°C or lower),[59,60] due to high content of ATH that counteracts the plasticization ability of DOP.

The glass transition step for annealed materials was analyzed with DSC (Figure 9). Upon annealing, plasticizer evaporates and T_g rises toward the value for virgin, unplasticized PVC (~81°C[61]). Interestingly, none of the MMTs imposes any significant changes in T_g or Δc_p before annealing (Table IV). The PVC/Na-3 nanocomposite has now T_g higher than the reference by 8°C, presumably due to confinement effects similar to those reported in PVC thin films.[62] The organo-modified MMT has a similar but weaker effect. It may be explained by the plasticization/lubrication ability of organic chains of the modifier.

The melting behavior after rubbery annealing analyzed with DSC and TOPEM® is shown in Figures 9 and 10, respectively. The materials, upon annealing, show small shift in the melting point to higher temperatures and only slight changes in the heat of fusion ΔH_m (Table IV). Apparently, the annealing process allows for reorganization of polymer macrochains and thus increases the crystallinity, but only moderately,[63] while the formed crystals become more stable. Interestingly, the nonmodified MMT enhances crystallinity, presumably acting as

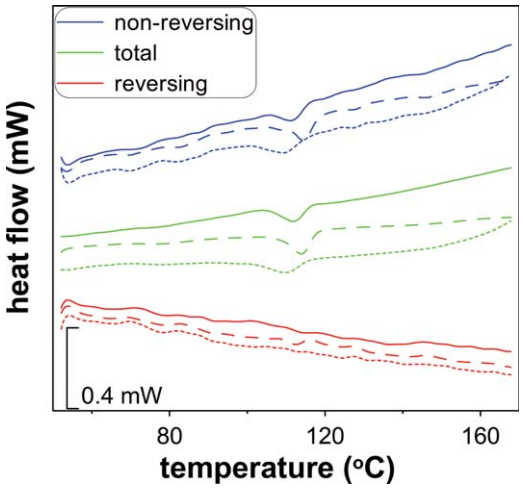

Figure 10. TOPEM® results for PVC and its nanocomposites: solid, PVC; dashed, PVC/Na-3; dotted, PVC/SE-3 (2°/min). [Color figure can be viewed in the online issue, which is available at wileyonlinelibrary.com.]

nucleating agent, while the organo-modified one seems to inhibit order and thus crystal formation.

CONCLUSIONS

In this work, PVC/MMT nanocomposites prepared by melt blending with sodium substituted, and organically modified montmorillonite were investigated with respect to their weathering performance. Laboratory aging tests were carried out to investigate the long-term behavior of PVC/MMT nanocomposites in comparison to virgin PVC blend.

Thermal aging causes loss of plasticizer and formation of different species built with polyene sequences and carbonyl groups, through several subsequent reactions. The materials change color, especially those with organo-modified MMT addition. Presumably, decomposition of organic modifier inside the MMT structure promotes dehydrochlorination of PVC. On the other hand, the nonmodified MMT has only slight influence on the PVC degradation and thus limited discoloration, under thermal aging. Based on the results obtained one can suggest that hydroxyl groups in the structure of PVC additives (ATH, MMT, and calcium stearate) are able to trap radicals that initiate dehydrochlorinaton.

Upon artificial weathering, both yellowing and photobleaching occurred, due to polyene sequences formation and photooxidation processes involving carbonyls species, respectively. It was also observed that the loss of additives from polymer matrix due to UV aging, involving mainly a loss of plasticizer and migration of inorganic additives to the surface of nanocomposite.

Comparing both, thermal and artificial weathering, it can be concluded that the different mechanism of the degradation is observed. In the thermal aging, the aggregation of the material due to loss of plasticizer and decomposition of organic modifier of MMT is the main reason for color and structural changes. Meanwhile, during weathering the migration of inorganic components, and rapid loss of the plasticizer cause numbered micropores formation.

The addition of MMT significantly influences the PVC stability. The most stable composite is the material containing nonmodified MMT, because it presents similar to the PVC thermal behavior and slightly improved surface stability.

The annealing of PVC composites at 70°C leads to reorganization of the polymer macrochains and loss of the plasticizer, which was also observed during thermal degradation at 180°C. On the basis of change in heat capacity during glass transition, it can be stated that materials with nonmodified MMT are characterized by stronger molecular interactions between the polymer composition and the clay (MMT) platelets, in comparison to the PVC/OMMT nanocomposites.

The addition of MMT to polymer matrix influences the mechanism of polymer matrix's weathering. The main result of the artificial weathering test was yellowing and darkening of the material.

ACKNOWLEDGMENTS

This work was financed by the Polish Ministry of Science and Higher Education under contract no. 0583/R/2/T02/07/02. The authors are grateful to Dr. Slawomir Kuberski and Ms. Aneta Bomba-Stolarek (Faculty of Process and Environmental Engineering, Technical University of Lodz, Poland) for the kind use of weathering equipment, and to Mr. Beat Flachsmann from Mettler-Toledo for permission to use TOPEM® DSC823^e. Valuable discussions with Dr. Konstantinos Raftopoulos are gratefully acknowledged.

REFERENCES

1. Coaker, W. In PVC Handbook; Wilkes, C. E., Summers, J. W., Daniels, C. A., Eds.; Carl Hanser Verlag: Munich, **2005**; Chapter *10*, p 329.
2. Babinsky, R. *J. Vinyl Addit. Technol.* **2007**, *13*, 1.
3. Wypych, G. PVC Degradation & Stabilization; ChemTec Publishing: Toronto, **2008**.
4. Ishida, H.; Campbell, S.; Blackwell, J. *Chem. Mater.* **2000**, *12*, 1260.
5. Wang, D.; Parlow, D.; Yao, Q.; Wilkie, C. *J. Vinyl Addit. Technol.* **2001**, *7*, 203.
6. Lepoittevin, B.; Pantoustier, N.; Devalckenaere, M.; Alexandre, M.; Calberg, C.; Jérôme, R.; Henrist, C.; Rulmont, A.; Dubois, P. *Polymer* **2003**, *44*, 2033.
7. Beyer, G. *Polym. Adv. Technol.* **2008**, *19*, 485.
8. Francis, N.; Schmidt, D. Improved lead-free wire and cable insulation performance using nanocomposites. Technical Report No. 58, University of Massachusetts, **2006**.
9. Wang, D.; Wilkie, C. *J. Vinyl Addit. Technol.* **2002**, *8*, 238.
10. Bibi, N.; Sarwar, M. I.; Ishaq, M.; Ahmad, Z. *Polym. Polym. Compos.* **2007**, *15*, 313.
11. Gong, F.; Feng, M.; Zhao, C.; Zhang, S.; Yang, M. *Polym. Degrad. Stab.* **2004**, *84*, 289.

12. Obłój-Muzaj, M.; Zielecka, M.; Kozakiewicz, J.; Abramowicz, A.; Szulc, A.; Domanowski, W. *Polimery* **2006**, *51*, 133.
13. Yang, D.-Y.; Liu, Q.-X.; Xie, X.-L.; Zeng, F.-D. *J. Therm. Anal. Calorim.* **2006**, *84*, 355.
14. Pagacz, J.; Pielichowski, K. *J. Vinyl Addit. Technol.* **2009**, *15*, 61.
15. Benderly, D.; Osorio, F.; Ijdo, W. L. *J. Vinyl Addit. Technol.* **2008**, *14*, 155.
16. White, J. R.; Turnbull, A. *J. Mater. Sci.* **1994**, *29*, 584.
17. Wypych, W., Ed. Handbook of Material Weathering, 4th ed.; ChemTec Publishing: Toronto, **2008**.
18. Gervat, L.; Morel, P. *J. Vinyl Addit. Technol.* **1996**, *2*, 37.
19. Girois, S.; Schipper, P. S. *J. Vinyl Addit. Technol.* **2001**, *7*, 61.
20. Lemaire, J.; Siampiringue, N.; Chaigneau, R.; Delprat, P.; Parmeland, G.; Dabin, P.; Spriet, C. *J. Vinyl Addit. Technol.* **2000**, *6*, 69.
21. Gumargalieva, K. Z.; Ivanov, V. B.; Zaikov, G. E.; Moiseev, Ju. V.; Pokholok, T. V. *Polym. Degrad. Stab.* **1996**, *52*, 73.
22. The behaviour of PVC in landfill, European Commission DGXI.E.3, Final report 2000. Available at: http://ec.europa.eu/environment/waste/studies/pvc/landfill.pdf (accessed September 22, 2014).
23. Mersiowsky, I. *J. Vinyl Addit. Technol.* **2002**, *8*, 36.
24. Sterky, K.; Hjertberg, T.; Jacobson, H. *Polym. Degrad. Stab.* **2009**, *94*, 1564.
25. Awad, W. H.; Beyer, G.; Benderly, D.; Ijdo, W. L.; Songtipya, P.; del Mar Jimenez-Gasco, M.; Manias, E.; Wilkie, C. A. *Polymer* **2009**, *50*, 1857.
26. Saeedi, M.; Ghasemi, I.; Karrabi, M. *Iran. Polym. J.* **2011**, *20*, 423.
27. Du, J.; Wang, D.; Wilkie, D. W.; Wilkie, C. A.; Wang, J. *Polym. Degrad. Stab.* **2003**, *79*, 319.
28. Peprnicek, T.; Duchet, J.; Kovarova, L.; Malac, J.; Gerard, J. F.; Simonik, J. *Polym. Degrad. Stab.* **2006**, *91*, 1855.
29. Pagacz, J.; Pielichowski, K. In Proceedings of the 5th Modern Polymeric Materials for Environmental Applications, Krakow, Poland, May 15–17, **2013**, p 95.
30. Pagacz, J.; Pielichowski, K. In Proceedings of the 4th Modern Polymeric Materials for Environmental Applications, Krakow, Poland, December 1–3, **2010**, p 17.
31. Khemici, M. W.; Gouraria, A.; Bendaoud, M. *Int. J. Polym. Anal. Charact.* **2006**, *11*, 101.
32. Alves, N. M.; Mano, J. F.; Balaguer, E.; Meseguer, J. M.; Gomez Ribelles, J. L. *Polymer* **2002**, *43*, 4111.
33. Schawe, J. E. K.; Heter, T.; Hertz, C.; Alig, I.; Lellinger, D. *Thermochim. Acta* **2006**, *446*, 147.
34. Berns, R. S. In Billmeyer and Saltzman's Principles of Color Technology, 3rd ed.; Berns, R. S., Ed.; Wiley: New York, **2000**.
35. Balköse, D.; Egbuchunam, T. O.; Okieimen, F. E. *J. Vinyl Addit. Technol.* **2008**, *14*, 65.
36. García-Castañeda, C.; Benavides, R.; Martínez-Pardo, M. E.; Uribe, R. M.; Carrasco-Ábrego, H.; Martínez, G. *Radiat. Phys. Chem.* **2010**, *79*, 335.
37. Beltran, M.; Marcilla, A. *Eur. Polym. J.* **1997**, *33*, 1271.
38. Wypych, G. Handbook of Polymers; ChemTec Publishing: Toronto, **2012**.
39. Garcia, D.; Black, J. *J. Vinyl Addit. Technol.* **1999**, *5*, 81.
40. Bockhorn, H.; Hornung, A.; Hornung, U. *J. Anal. Appl. Pyrol.* **1999**, *50*, 77.
41. Wan, C.; Zhang, Y.; Zhang, Y. *Polym. Test.* **2004**, *23*, 299.
42. Quill, J. P.; Ledgerwood, P. In Proceedings of 2nd European Weathering Symposium, Gothenburg, Germany, June 2005, p 25.
43. Ito, R.; Seshimo, F.; Haishima, Y.; Hasegawa, C.; Isama, K.; Yagami, T.; Nakahashi, K.; Yamazaki, H.; Inoue, K.; Yoshimura, Y.; Saito, K.; Tsuchiya, T.; Nakazawa, H. *Int. J. Pharm.* **2005**, *303*, 104.
44. Carlsson, D. J.; Krzymien, M.; Worsfold, D. J.; Day, M. *J. Vinyl Addit. Technol.* **1997**, *3*, 100.
45. Matuana, L. M.; Kamden, D. P. *Polym. Eng. Sci.* **2002**, *42*, 1657.
46. Krzymien, M. E.; Day, M.; Worsfold, J.; Carlsson, D. *J. Macromol. Symp.* **1997**, *115*, 27.
47. Holle, S.; Laurent, J.-L. *Polym. Degrad. Stab.* **1997**, *55*, 141.
48. Owen, E. D.; Pasha, I.; Moayyedi, F. *J. Appl. Polym. Sci.* **1980**, *25*, 2331.
49. Owen, E. D.; Read, R. L. *J. Polym. Sci. Polym. Chem. Ed.* **1979**, *17*, 2719.
50. Andrady, A. L.; Fueki, K.; Torika, A. *J. Appl. Polym. Sci.* **1990**, *39*, 763.
51. Shashoua, Y. R. *Polym. Degrad. Stab.* **2003**, *81*, 29.
52. Karmalm, P.; Hjertberg, T.; Jansson, A.; Dahl, R. *Polym. Degrad. Stab.* **2009**, *94*, 2275.
53. Chen, C.-H.; Teng, C.-C.; Yang, C.-H. *J. Polym. Sci. Part B: Polym. Phys.* **2005**, *43*, 1465.
54. Jonsson, S.; Ejlertsson, J.; Svensson, B. H. *Waste Manage.* **2003**, *23*, 641.
55. Real, L. E. P.; Ferraria, A. M.; Rego, A. M. B. *Polym. Test.* **2007**, *26*, 77.
56. Ito, M.; Nagai, K. *Polym. Degrad. Stab.* **2007**, *92*, 260.
57. Pagacz, J. Selected aspects of the preparation and characterization of poly(vinyl chloride)/montmorillonite nanocomposites (PVC/MMT). Ph.D. Thesis, Cracow University of Technology, Krakow, October **2013**.
58. Pagacz, J.; Pielichowski, K. *J. Therm. Anal. Calorim.* **2013**, *111*, 1571.
59. Stuart, A.; McCallum, M. M.; Fan, D.; LeCaptain, D. J.; Lee, C. Y.; Mohanty, D. K. *Polym. Bull.* **2010**, *65*, 589.
60. Collins, E. A.; Daniels, C. A.; Witenhafer, D. E. In Polymer Handbook; Brandrup, J., Immergut, E. H., Grulke, E. A., Eds.; Wiley: New York, **1999**, p V/70.
61. Gomez Ribelles, J. L.; Diaz-Calleja, R.; Fergusson, R.; Cowie, J. M. G. *Polymer* **1987**, *28*, 2262.
62. Grohens, Y.; Sacristan, J.; Hamon, L.; Reinecke, H.; Mijangos, C.; Guenet, J. M. *Polymer* **2001**, *42*, 6419.
63. Wang, D.; Parlow, D.; Yao, Q.; Wilkie, C. A. *J. Vinyl Addit. Technol.* **2002**, *8*, 139.